

Self-consistent micromagnetic simulations including spin-diffusion effects

Claas Abert^{*1}, Michele Ruggeri², Florian Bruckner¹, Christoph Vogler³, Gino Hrkac⁴, Dirk Praetorius², and Dieter Suess¹

¹*Christian Doppler Laboratory of Advanced Magnetic Sensing and Materials, Institute of Solid State Physics, Vienna University of Technology, Austria*

²*Institute for Analysis and Scientific Computing, Vienna University of Technology, Austria*

³*Institute of Solid State Physics, Vienna University of Technology, Austria*

⁴*College of Engineering, Mathematics and Physical Sciences, University of Exeter, United Kingdom*

April 27, 2022

Abstract

We implement a finite-element scheme that solves the Landau-Lifshitz-Gilbert equation coupled to a diffusion equation accounting for spin-polarized currents. The latter solves for the spin accumulation not only in magnetic materials but also in nonmagnetic conductors. The presented method incorporates the model by Slonczewski for the description of spin torque in magnetic multilayers as well as the model of Zhang and Li for the description of current driven domain-wall motion. Furthermore it is able to do both resolve the time evolution of the spin accumulation or treat it in an adiabatic fashion by the choice of sufficiently large time steps.

Keywords: micromagnetics, finite-element method, spin torque, spin diffusion

*claas.abert@tuwien.ac.at

1 Introduction

The classical micromagnetic model describes ferromagnetic materials in the absence of electric currents. The governing equations are well understood and widely used for the analytical as well as numerical investigation of magnetic microstructures. However, in recent years the interaction of the magnetization with spin polarized currents, also referred to as spintronics, has gained a lot of interest. Due to the local character of this interaction it is a promising candidate for the improvement of magnetic storage technologies. Applications in the area of spintronics include the racetrack memory [1] and the STT-MRAM [2].

Different extensions to the micromagnetic model have been proposed to include the coupling of the magnetization to a spin polarized current. A model for the description of magnetic multilayers was first introduced by Slonczewski [3, 4] and Berger [5]. The model describes a current flow perpendicular to a layer system consisting of a fixed magnetic layer, a nonmagnetic layer and a free magnetic layer. The current is assumed to pick up its spin polarization in the fixed layer and exert a torque on the magnetization in the free layer. While this model is successfully applied to MRAM like structures it is not suited for the description of current driven domain-wall motion where no magnetic fixed layer is involved.

A more general model to spin polarized currents introduces a spin-accumulation field that is bidirectionally coupled to the magnetization [6, 7]. The explicit computation of the spin accumulation can be avoided by neglecting spin-diffusion effects and treating the spin accumulation in an adiabatic fashion [8]. This simplified model is able to describe domain-wall motion, but fails in the description of multi-layer structures.

We implement a finite-element scheme for the solution of the full spin-diffusion model that has been shown to be unconditionally convergent [9]. We perform numerical experiments and compare the results with the simplified models by Slonczewski and Zhang et al.

This paper is organized as follows. In Sec. 2 and 3 the spin-diffusion model and its discretization are introduced. Sec. 4 discusses the implementation and in Sec. 5 the model is tested and compared to other spin-polarization models.

2 Model

The magnetization dynamics are described by the Landau-Lifshitz-Gilbert equation

$$\frac{\partial \mathbf{m}}{\partial t} = -\gamma \mathbf{m} \times (\mathbf{h}_{\text{eff}} + \frac{c}{\mu_0} \mathbf{s}) + \alpha \mathbf{m} \times \frac{\partial \mathbf{m}}{\partial t} \quad (1)$$

where \mathbf{m} is the normalized magnetization, γ is the gyromagnetic ratio, α is the Gilbert damping and \mathbf{h}_{eff} is the effective field given by the negative variational derivative of the total free energy U

$$\mathbf{h}_{\text{eff}} = -\frac{1}{\mu_0 M_s} \frac{\delta U}{\delta \mathbf{m}} \quad (2)$$

where μ_0 is the magnetic constant and M_s is the saturation magnetization. Contributions to the effective field usually include the exchange field given by

$$\mathbf{h}_{\text{exch}} = \frac{2A}{\mu_0 M_s} \Delta \mathbf{m} \quad (3)$$

with the material dependent exchange constant A and the demagnetization field $\mathbf{h}_{\text{demag}} = -\nabla u$ generated by a magnetic region ω with the potential u defined by

$$\Delta u = M_s \nabla \cdot \mathbf{m} \quad \text{in } \omega \quad (4)$$

$$\Delta u = 0 \quad \text{in } \mathbb{R}^3 \setminus \omega \quad (5)$$

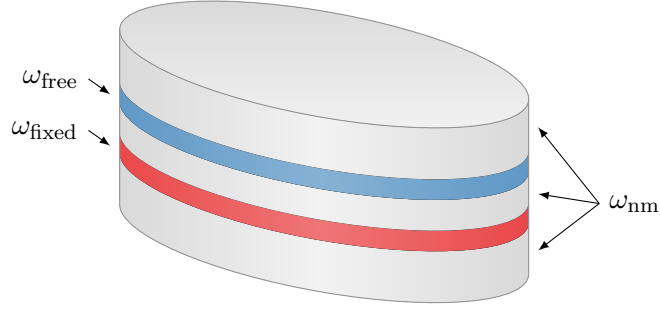


Figure 1: Typical multilayer structure for a spin torque nano-pillar. A magnetic fixed layer ω_{fixed} is separated from a magnetic free layer ω_{free} by a nonmagnetic spacer layer. The system is completed by two leads made of nonmagnetic material.

with jump and boundary conditions

$$[u]_{\partial\omega} = 0 \quad (6)$$

$$\left[\frac{\partial u}{\partial \mathbf{n}} \right]_{\partial\omega} = -M_s \mathbf{m} \cdot \mathbf{n} \quad (7)$$

$$u(\mathbf{x}) \rightarrow \mathcal{O}(1/|\mathbf{x}|) \quad \text{for } |\mathbf{x}| \rightarrow \infty \quad (8)$$

where \mathbf{n} is the outwards pointing unit normal. Further possible contributions are the external field \mathbf{h}_{ext} and the anisotropy field $\mathbf{h}_{\text{aniso}}$ whose analytical expression depends on the lattice structure of the magnetic material. The vector field \mathbf{s} in (1) is the spin accumulation generated by a spin current \mathbf{J}_s and c is the corresponding coupling constant. According to [10] the spin accumulation obeys the equation of motion

$$\frac{\partial \mathbf{s}}{\partial t} = -\nabla \cdot \mathbf{J}_s - 2D_0 \left[\frac{\mathbf{s}}{\lambda_{\text{sf}}^2} + \frac{\mathbf{s} \times \mathbf{m}}{\lambda_{\text{J}}^2} \right] \quad (9)$$

where D_0 is the diffusion constant, λ_{sf} is related to the spin-flip relaxation time τ_{sf} by $\lambda_{\text{sf}} = \sqrt{2D_0\tau_{\text{sf}}}$ and $\lambda_{\text{J}} = \sqrt{2hD_0/J_{\text{ex}}}$ with h being Planck's constant and J_{ex} being the exchange integral. The matrix-valued spin current \mathbf{J}_s is given by

$$\mathbf{J}_s = \frac{\beta\mu_{\text{B}}}{e} \mathbf{m} \otimes \mathbf{J}_e - 2D_0 [\nabla \mathbf{s} - \beta\beta' \mathbf{m} \otimes ((\nabla \mathbf{s})^T \mathbf{m})] \quad (10)$$

where μ_{B} is the Bohr magneton, e is the elementary charge and β and β' are dimensionless polarization parameters. Here $\nabla \mathbf{s}$ is defined as Jacobian of \mathbf{s} and the outer product $\mathbf{a} \otimes \mathbf{b}$ is defined as \mathbf{ab}^T .

Figure 1 shows a typical multilayer structure for the investigation of spin-torque effects. A magnetic fixed layer ω_{fixed} is separated from a magnetic free layer ω_{free} by a nonmagnetic layer ω_{nm} . Additional nonmagnetic layers above and beneath the magnetic layers serve as electrical contacts. The Landau-Lifshitz-Gilbert equation (1) is solved on the magnetic regions $\omega = \omega_{\text{fixed}} \cup \omega_{\text{free}}$ only. The spin accumulation is solved on the entire domain $\Omega = \omega \cup \omega_{\text{nm}}$.

3 Algorithm

The model introduced in the preceding section is discretized by an algorithm introduced in [9]. A splitting scheme is used to decouple the Landau-Lifshitz-Gilbert equation (1) from the

spin-accumulation equation (9). For each time step the Landau-Lifshitz-Gilbert equation is solved for a given spin-accumulation \mathbf{s}^k by a semi-implicit scheme introduced by Alouges in [11]. In a next step the updated magnetization \mathbf{m}^{k+1} is inserted into an implicit scheme for the spin-accumulation equation in order to compute \mathbf{s}^{k+1} . The complete algorithm for a time step τ reads:

1. Consider the orthogonal space \mathcal{T}_{m^k} to the magnetization \mathbf{m}^k defined by

$$\mathcal{T}_{m^k} = \{\mathbf{x} \in \mathbf{H}^1(\omega); \mathbf{x} \cdot \mathbf{m}^k = 0\} \quad (11)$$

with the Sobolev space \mathbf{H}^1 . Find $\mathbf{v}^k \in \mathcal{T}_{m^k}$ such that

$$\begin{aligned} \int_{\omega} (\alpha \mathbf{v}^k + \mathbf{m}^k \times \mathbf{v}^k) \cdot \mathbf{w} \, d\mathbf{x} + \frac{2\gamma A \theta \tau}{\mu_0 M_s} \int_{\omega} \nabla \mathbf{v}^k : \nabla \mathbf{w} \, d\mathbf{x} = \\ - \frac{2\gamma A}{\mu_0 M_s} \int_{\omega} \nabla \mathbf{m}^k : \nabla \mathbf{w} \, d\mathbf{x} + \gamma \int_{\omega} \mathbf{h}_{\text{explicit}} \cdot \mathbf{w} \, d\mathbf{x} \end{aligned} \quad (12)$$

for all $\mathbf{w} \in \mathcal{T}_{m^k}$ where $\mathbf{A} : \mathbf{B}$ defines the Frobenius inner product of two matrices. The parameter $\theta \in [0, 1]$ controls whether the exchange field is integrated explicitly ($\theta = 0$) or implicitly ($\theta = 1$). Following [12] all other effective-field contributions are summarized in $\mathbf{h}_{\text{explicit}}$ and integrated explicitly.

2. Compute \mathbf{m}^{k+1} by

$$\mathbf{m}_i^{k+1} = \frac{\mathbf{m}_i^k + \tau \mathbf{v}_i^k}{|\mathbf{m}_i^k + \tau \mathbf{v}_i^k|} \quad (13)$$

where the subscript i denotes the i th nodal value of the discretized field.

3. Find \mathbf{s}^{k+1} such that

$$\begin{aligned} \int_{\Omega} d_t \mathbf{s}^{k+1} \cdot \boldsymbol{\zeta} \, d\mathbf{x} + 2D_0 a(\mathbf{s}^{k+1}, \boldsymbol{\zeta}) = \\ \frac{\beta \mu_B}{e} \int_{\omega} [\mathbf{m}^{k+1} \otimes \mathbf{J}_e^{k+1}] : \nabla \boldsymbol{\zeta} \, d\mathbf{x} - \frac{\beta \mu_B}{e} \int_{\partial\Omega \cap \partial\omega} (\mathbf{J}_e^{k+1} \cdot \mathbf{n})(\mathbf{m}^{k+1} \cdot \boldsymbol{\zeta}) \, d\mathbf{x} \end{aligned} \quad (14)$$

for all $\boldsymbol{\zeta} \in \mathbf{H}^1(\Omega)$ where \mathbf{n} is the outwards pointing facet normal. Furthermore $d_t \mathbf{s}^{k+1} = (\mathbf{s}^{k+1} - \mathbf{s}^k)/\tau$ and the bilinear form $a(\boldsymbol{\zeta}_1, \boldsymbol{\zeta}_2)$ is defined as

$$\begin{aligned} a(\boldsymbol{\zeta}_1, \boldsymbol{\zeta}_2) = \frac{1}{\lambda_{\text{sf}}^2} \int_{\Omega} \boldsymbol{\zeta}_1 \cdot \boldsymbol{\zeta}_2 \, d\mathbf{x} + \int_{\Omega} \nabla \boldsymbol{\zeta}_1 : \nabla \boldsymbol{\zeta}_2 \, d\mathbf{x} \\ - \beta \beta' \int_{\omega} [\mathbf{m}^{k+1} \otimes ((\nabla \boldsymbol{\zeta}_1)^T \mathbf{m}^{k+1})] : \nabla \boldsymbol{\zeta}_2 \, d\mathbf{x} + \frac{1}{\lambda_J^2} \int_{\omega} (\boldsymbol{\zeta}_1 \times \mathbf{m}^{k+1}) \cdot \boldsymbol{\zeta}_2 \, d\mathbf{x} \end{aligned} \quad (15)$$

according to [9].

The vector fields \mathbf{m} , \mathbf{s} , \mathbf{v} and test functions \mathbf{w} , $\boldsymbol{\zeta}$ are discretized with piecewise affine, globally continuous functions constructed on a tetrahedral tessellation of the domain Ω . Material constants that differ from subdomain to subdomain, e.g. the diffusion constant D_0 , are discretized by piecewise constant functions.

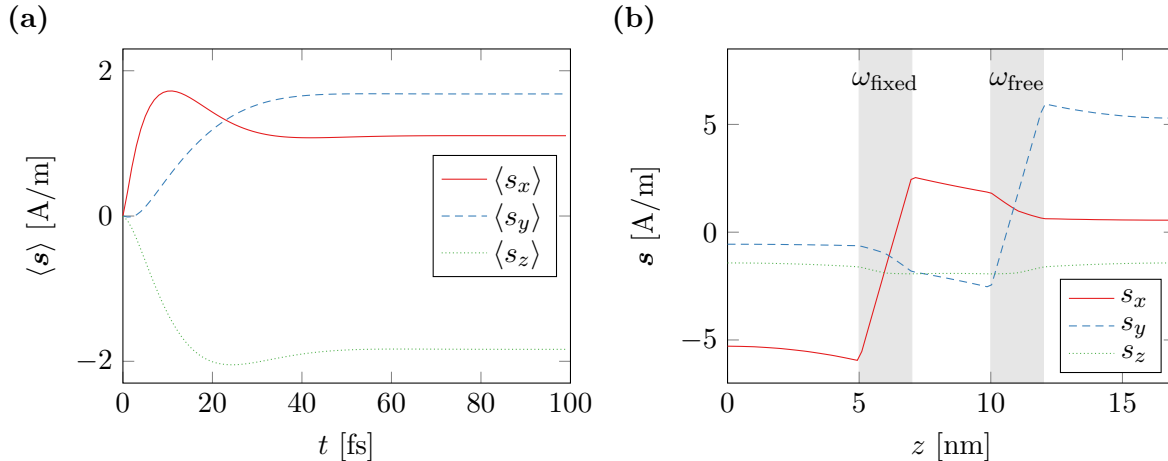


Figure 2: Spin accumulation in a magnetic multilayer structure. The magnetization is homogeneous and in-plane within the magnetic regions. (a) Spatially averaged components of the spin diffusion in the free layer during relaxation. (b) Spin diffusion in equilibrium along the the z -axis of the multilayer.

4 Implementation

The presented algorithm is implemented within the finite-element micromagnetic code `magnum.fe` [13, 14]. `magnum.fe` uses FEniCS [15] for the assembly and solution of the finite-element systems. The linear systems arising from discretization of (12) and (14) are solved iteratively by a GMRES solver. The demagnetization-field problem (4)–(8) can be either solved by a shell-transformation method, see [16, 17], or a hybrid finite-element boundary-element method, see [18]. For the latter method the BEM++ package is used [19].

5 Numerical Experiments

As a first test the time development of the spin diffusion for a fixed magnetization configuration is computed. An ellipsoidal multilayer structure as pictured in Fig. 1 with axis lengths 130×70 nm and layer thicknesses (5, 2, 3, 2, 5) nm is considered. In the following the coordinate system is chosen such that the long and short axes of the ellipse align with the x and y -axis respectively. The diffusion constant in the magnetic layers ω_{free} and ω_{fixed} is set to $D_0 = 1 \times 10^{-3} \text{ m}^2/\text{s}$. In the nonmagnetic region the diffusion constant is chosen as $D_0 = 5 \times 10^{-3} \text{ m}^2/\text{s}$. The remaining constants are $\lambda_{\text{sf}} = 10$ nm, $\lambda_{\text{J}} = 2$ nm, $\beta = 0.9$, $\beta' = 0.8$, and $c = 3.125 \times 10^{-3} \text{ N/A}^2$. The magnetization \mathbf{m} is initialized homogeneously parallel to the x -axis in the fixed layer and parallel to y -axis in the free layer. Equation (14) is then solved repeatedly for a homogeneous current density perpendicular to the layers $\mathbf{J}_e = (0, 0, 10^{11}) \text{ A/m}^2$, a time step $\tau = 1$ fs and an initial spin accumulation of $\mathbf{s} = 0$.

Figure 2a shows the simulation results. The system relaxes within approximately 70 fs. This time scale is 2 orders of magnitude below the typical reaction time of the magnetization \mathbf{m} . Hence the magnetization dynamics may be accurately described by assuming the spin accumulation to be in equilibrium at any times [6]. However, the presented integration scheme for the spin accumulation is able to handle very large time steps due to its implicit nature and the linearity of the problem. In fact it shows that even for an initial spin accumulation of $\mathbf{s} = 0$ two integration steps with $\tau = 1$ ps are sufficient to obtain the equilibrium state accurately.

When moving from one magnetization configuration to the next during time integration of the Landau-Lifshitz-Gilbert equation, a single integration step of the spin accumulation yields the equilibrium state. The presented algorithm is thus well suited for investigating the time evolution of both the spin diffusion using time steps $\tau \approx 1$ fs as well as the magnetization using time steps $\tau \approx 1$ ps.

Figure 2b shows the equilibrium spin accumulation \mathbf{s} on the z -axis in the middle of the multilayer structure. From (9) it is clear, that the source of the spin accumulation is the spatial change of the magnetization \mathbf{m} . Since the magnetization is homogeneous within the magnetic regions, the spin accumulation is expected to be generated at the layer interfaces and diffuse into the regions which is well reflected by the simulation results.

5.1 Comparison to Model by Slonczewski

An established model for the description of spin-torque effects in magnetic multilayers was introduced by Slonczewski in [4]. The fixed layer in this model is homogeneously magnetized and fixed in the sense that the magnetization does not change in time. The electric current \mathbf{J}_e is assumed to pick up its spin polarization in the fixed layer and then interact with the free layer by an additional term to the Landau-Lifshitz-Gilbert equation

$$\mathbf{N} = \eta(\theta) \frac{\hbar}{2e} \frac{J_e}{d} \mathbf{m} \times (\mathbf{m} \times \mathbf{M}). \quad (16)$$

Here \mathbf{M} denotes the normalized magnetization of the fixed layer, d is the thickness of the free layer and θ is the angle between the magnetization in the fixed layer and the magnetization with $\cos(\theta) = \mathbf{M} \cdot \mathbf{m}$. The additional contribution \mathbf{N} is added to the right-hand side of the Landau-Lifshitz-Gilbert equation (1) without spin-accumulation \mathbf{s} . The angular coefficient $\eta(\theta)$ for structures with equal height fixed and free layers is given by

$$\eta(\theta) = \frac{q}{A + B \cos(\theta)} \quad (17)$$

where q , A , and B are constants that depend on the geometry and the material parameters of the system. Consider the previously described ellipsoidal multilayer structure with the magnetization being homogeneous and in-plane in both the fixed layer and the free layer. In this case the additional torque term in the free layer (16) is expected to be in-plane with a magnitude given by

$$N \propto \sin(\theta) \frac{q}{A + B \cos(\theta)}. \quad (18)$$

Figure 3a shows the magnitude of the torque term $\mathbf{m} \times \mathbf{s}$ as computed by the spin-accumulation model. The result is split into the in-plane magnitude $(\mathbf{m} \times \mathbf{s})_{xy}$ and the out-of-plane magnitude $(\mathbf{m} \times \mathbf{s})_z$. Furthermore the in-plane magnitude is fitted with the magnitude as predicted by Slonczewski (18). Since the system is overdefined for fitting, q is set to 1 and A and B are chosen as fitting parameters. As seen in Fig. 3a the fit is very accurate. The relative fitting error for both A and B is well below 10^{-6} . Not only the in-plane magnitude, but also the in-plane angle of the torque term shows excellent accordance to the spin-torque model of Slonczewski as depicted in Fig. 3b. However, the spin-accumulation model predicts a non-negligible out-of-plane torque that cannot be explained by the simplified model.

As pointed out in [20] the expression for the angular coefficient (17) only holds for the symmetric case of equal height fixed and free layer. For the general case the angular coefficient reads

$$\eta(\theta) = \frac{q_+}{A + B \cos(\theta)} + \frac{q_-}{A - B \cos(\theta)}. \quad (19)$$

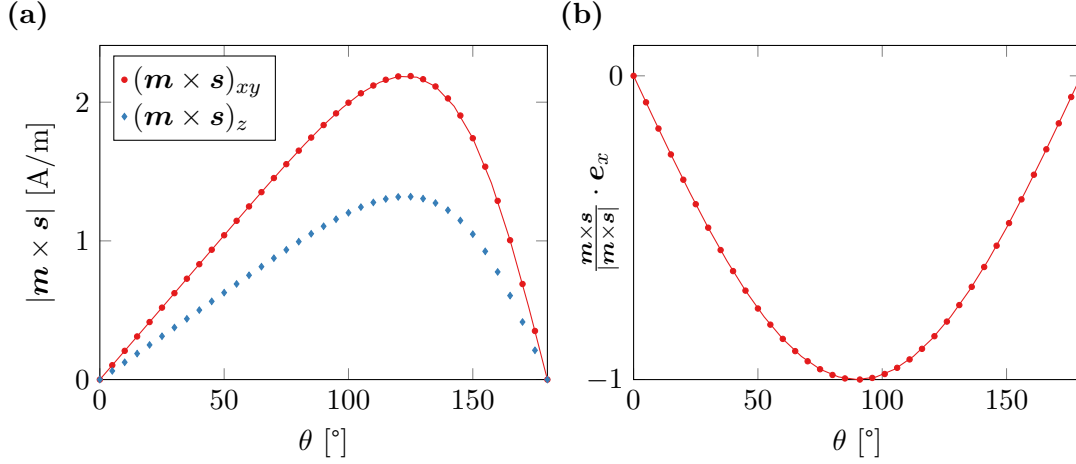


Figure 3: Spin torque $\mathbf{m} \times \mathbf{s}$ in a magnetic multilayer structure with layer thicknesses (5, 2, 3, 2, 5) nm and $\lambda_J = 2$ nm. The magnetization in the fixed layer and the free layer is homogeneous, in-plane, and tilted by θ . The marks represent values computed with the spin diffusion model and the lines show a fit with the model of Slonczewski. (a) In-plane and out-of-plane component of the equilibrium spin torque. (b) In-plane angle of the spin-torque with respect to the magnetization direction in the fixed layer.

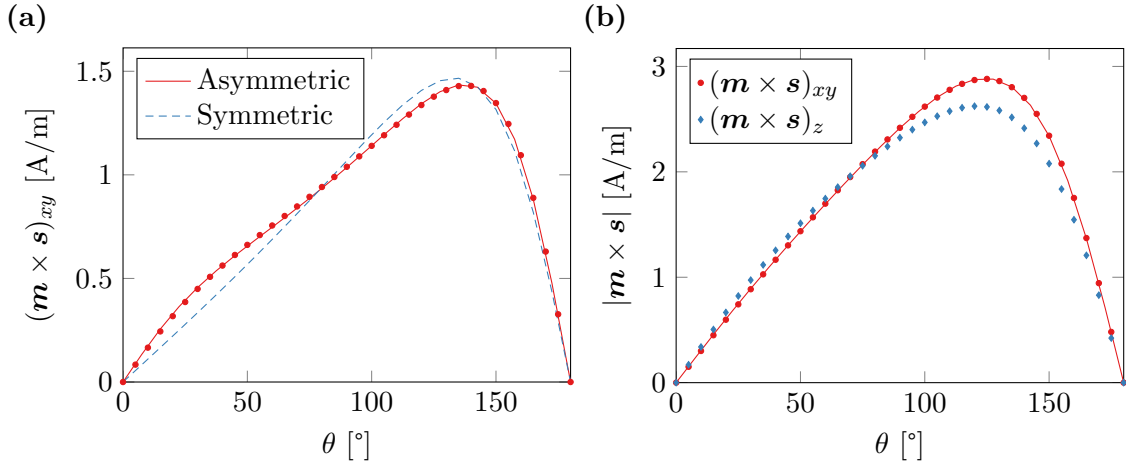


Figure 4: Spin torque $\mathbf{m} \times \mathbf{s}$ in a magnetic multilayer structure with layer thicknesses (5, 10, 3, 2, 5) nm. The marks represent values computed with the spin diffusion model and the lines show a fit with the model of Slonczewski. (a) In-plane spin torque for $\lambda_J = 1$ nm. The data is fitted with both a symmetric and an asymmetric model. (b) In-plane and out-of-plane component of the spin torque for $\lambda_J = 2$ nm.

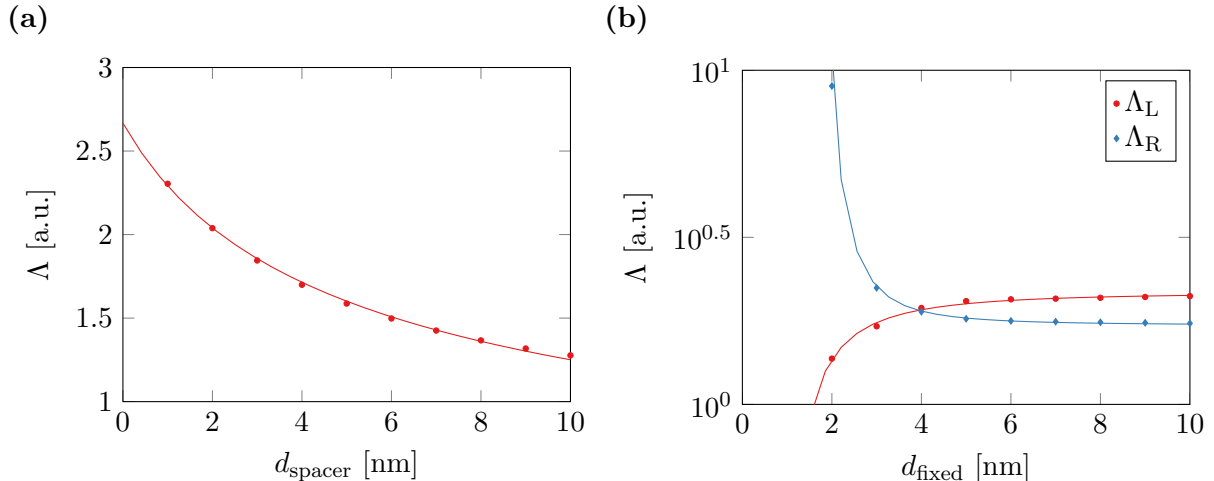


Figure 5: Dependence of the fitting parameter Λ on the geometry of a multilayer structure with layer thicknesses (5, 2, 3, 2, 5) nm. (a) Variation of the spacer thickness, i.e. (5, d_{spacer} , 2, 5) nm. (b) Variation of the fixed-layer thickness, i.e. (5, d_{fixed} , 3, 2, 5) nm.

Figure 4a shows the computed in-plane torque for $\lambda_J = 1$ nm together with fitted curves for the symmetric model (17) and the asymmetric model (19) respectively. The computed torque is well fitted by the asymmetric model with relative errors below 2×10^{-4} , while the symmetric model obviously fails in the correct description of the asymmetric problem. However, again the spin-diffusion model predicts a z -component of the torque that is not described by the spin-torque model of Slonczewski. The ratio of in-plane torque to out-of-plane torque for a given structure is largely influenced by the choice of λ_J . Choosing large values for λ_J leads to high out-of-plane components of the torque, see Fig. 4b.

The coefficients A , B , q , q_+ , and q_- depend, among other things, on the geometry of the system. In the following the dependence of these constants on the thickness of the nonmagnetic layer and the fixed layer is investigated in detail. A physically motivated choice for the right-hand-side coefficients in (19) is introduced in [20]

$$q_{\pm} = \frac{1}{2} \left[P_L \Lambda_L^2 \sqrt{\frac{\Lambda_R^2 + 1}{\Lambda_L^2 + 1}} \pm P_R \Lambda_R^2 \sqrt{\frac{\Lambda_L^2 + 1}{\Lambda_R^2 + 1}} \right] \quad (20)$$

$$A = \sqrt{(\Lambda_L^2 + 1)(\Lambda_R^2 + 1)} \quad (21)$$

$$B = \sqrt{(\Lambda_L^2 - 1)(\Lambda_R^2 - 1)} \quad (22)$$

where Λ_L , Λ_R , P_L , and P_R describe the properties of the fixed and the free layer respectively. For symmetric structures, i.e. $\Lambda_L = \Lambda_R$ and $P_L = P_R$, (19) reduces to

$$\eta(\theta) = \frac{P\Lambda^2}{(\Lambda^2 + 1) + (\Lambda^2 - 1)\cos(\theta)}. \quad (23)$$

Figure 5a shows the dependence of Λ from the thickness of the spacer layer in a symmetric multilayer structure. The simulation results are well fitted with a shifted reciprocal square root $\Lambda(d) \propto 1/\sqrt{\Delta + d}$. The dependence of Λ_L and Λ_R on the thickness of the fixed layer in an asymmetric structure is depicted in Fig. 5b. Both coefficients are well fitted by a shifted reciprocal square function $\Lambda_{L/R}(d) = X + Y/(\Delta + d)$ with X , Y , and Δ being fit parameters.

The model of Slonczewski provides a straightforward way to deal with multilayer structures. However, it is obviously not suited for the description of spin-torque effects in smoothly varying magnetization configurations since it requires a separated fixed layer to generate the spin polarization of the current.

5.2 Comparison to Model by Zhang and Li

An alternative spin-torque model was introduced by Zhang and Li in [8]. The model of Zhang and Li can be derived from the spin-diffusion model (9) by introducing the following simplifications: The spin diffusion \mathbf{s} is assumed to vary little in space and thus terms involving $\nabla \mathbf{s}$ are omitted. The electric current is assumed to be divergence free within the simulated regions, i.e. $\nabla \cdot \mathbf{J}_e = 0$. Furthermore the spin accumulation is assumed to be in equilibrium at all times, i.e. $\partial \mathbf{s} / \partial t = 0$. With these assumptions (9) reads

$$\frac{\partial \mathbf{s}}{\partial t} = -\frac{\beta \mu_B}{e} \nabla \cdot (\mathbf{m} \otimes \mathbf{J}_e) - 2D_0 \left[\frac{\mathbf{s}}{\lambda_{sf}^2} + \frac{\mathbf{s} \times \mathbf{m}}{\lambda_J^2} \right] \quad (24)$$

$$= -\frac{\beta \mu_B}{e} (\mathbf{J}_e \cdot \nabla) \mathbf{m} - 2D_0 \left[\frac{\mathbf{s}}{\lambda_{sf}^2} + \frac{\mathbf{s} \times \mathbf{m}}{\lambda_J^2} \right] \quad (25)$$

$$= 0. \quad (26)$$

Applying basic vector algebra and $\mathbf{m} \cdot \mathbf{m} = 1$ yields

$$\mathbf{m} \times \mathbf{s} = \frac{1}{1 + \xi^2} \frac{\lambda_J^2 \beta \mu_B}{2D_0 e} \left(-\mathbf{m} \times [\mathbf{m} \times (\mathbf{J}_e \cdot \nabla) \mathbf{m}] - \xi \mathbf{m} \times (\mathbf{J}_e \cdot \nabla) \mathbf{m} \right) \quad (27)$$

with the degree of non-adiabacity $\xi = \lambda_J^2 / \lambda_{sf}^2$. The obvious advantage of this method is that the spin accumulation does not have to be calculated explicitly. The spin torque $\mathbf{m} \times \mathbf{s}$ does only depend on the magnetization \mathbf{m} and other known entities and can be added directly to the Landau-Lifshitz-Gilbert equation (1).

Figure 6a shows the magnetization configuration \mathbf{m} for a Néel-wall in a $600 \times 100 \times 2$ nm thin film with the material parameters of permalloy ($M_s = 8 \times 10^5$ A/m, $A = 1.3 \times 10^{-11}$ J/m, $K = 0$) as computed with magnum.fe. The corresponding spin torque $\mathbf{m} \times \mathbf{s}$ is computed once by relaxation of the spin-diffusion model (9), see Fig. 6b, and once by the model of Zhang and Li (27). The solution computed by the model of Zhang and Li shows a good agreement to the spin-diffusion solution with a relative L^2 error norm below 5×10^{-3} .

The assumption of a vanishing gradient of the spin accumulation $\nabla \mathbf{s}$, made in the model by Zhang and Li, is valid within the magnetic regions as discussed in [8]. However, at the interfaces of magnetic multilayers this assumption is violated. Hence the model by Zhang and Li is not suited for the description of such structures.

5.3 Standard Problem #5

A suitable benchmark for the interplay of magnetization and spin-diffusion dynamics is the micromagnetic standard problem #5 that was recently proposed by the μ Mag group, see [21]. A thin square of size $100 \times 100 \times 10$ nm with material parameters similar to permalloy is prepared in a vortex state. Then a constant current $J_e = 10^{12}$ A/m is applied in x -direction. The vortex core is expected to perform a damped rotation around a new equilibrium position. The spin-torque related constants in the problem definition are tailored to the model by Zhang and Li. Namely the degree of non-adiabacity ξ is given as well as a factor b that can be expressed in terms of spin-diffusion related constants as

$$b = \frac{1}{1 + \xi^2} \frac{\gamma c \lambda_J^2 \beta \mu_B}{2D_0 e \mu_0} \quad (28)$$

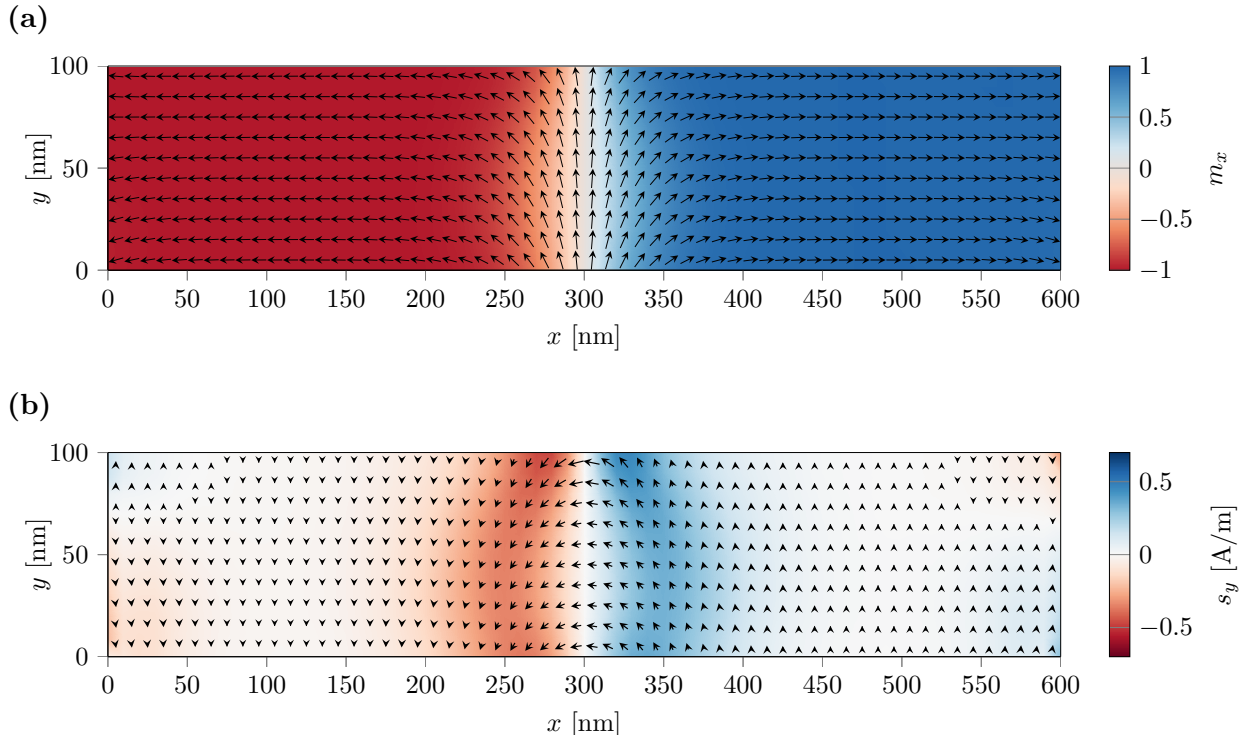


Figure 6: Néel domain wall in a thin strip of permalloy with dimensions $600 \times 100 \times 2$ nm. (a) Magnetization configuration. The x -component is color coded. (b) Spin-torque. The y -component is color coded.

according to (27). The spin-diffusion related parameters are chosen as $D_0 = 10^{-3} \text{ m/s}^2$, $\beta = 0.9$, $\beta' = 0.8$, $\lambda_{\text{sf}} = 10 \text{ nm}$, $\lambda_J \approx 2.236 \text{ nm}$, and $c \approx 3.155 \times 10^{-3} \text{ N/A}^2$. In fact λ_J and c are chosen such that $\xi = 0.05$ and $bJ = 72.17 \text{ m/s}$ is exactly fulfilled as required.

Figure 7 shows the simulation results in comparison to a reference solution computed with the finite-difference code MicroMagnum [22] that implements the model by Zhang and Li. The most notable difference is the shifted y -position of the vortex core in equilibrium. The authors believe that this is a result of the missing $\nabla \mathbf{s}$ terms in the model by Zhang and Li.

5.4 Switching of a Permalloy Multilayer Structure

As another test the current induced switching of a magnetic multilayer structure is simulated. The geometry considered is ellipsoidal with edge lengths $130 \times 70 \text{ nm}$ and layer thicknesses (3, 10, 3, 2, 3) nm. The material parameters in the magnetic layers are similar to those of permalloy, see preceding section. In the nonmagnetic layers the diffusion constant is set to $D_0 = 5 \times 10^{-3} \text{ m/s}^2$. Since the size of the ellipsoid is well under the single-domain limit, the energy of the system is minimal if the magnetization is aligned along the long axis of the ellipsoid in the magnetic layers. The thick and thin magnetic layers are referred to as fixed and free layer respectively, since the energy barrier for magnetic switching in the thick layer is higher than in the thin layer.

By applying a current perpendicular to the layer structure, the magnetization in the free layer can be switched. Figure 8a shows the hysteresis of the free layer for different currents. The shift of the curve is an expected consequence resulting from the strayfield coupling of the magnetic layers. An antiparallel configuration of the fixed and free layer is energetically favored over a parallel configuration.

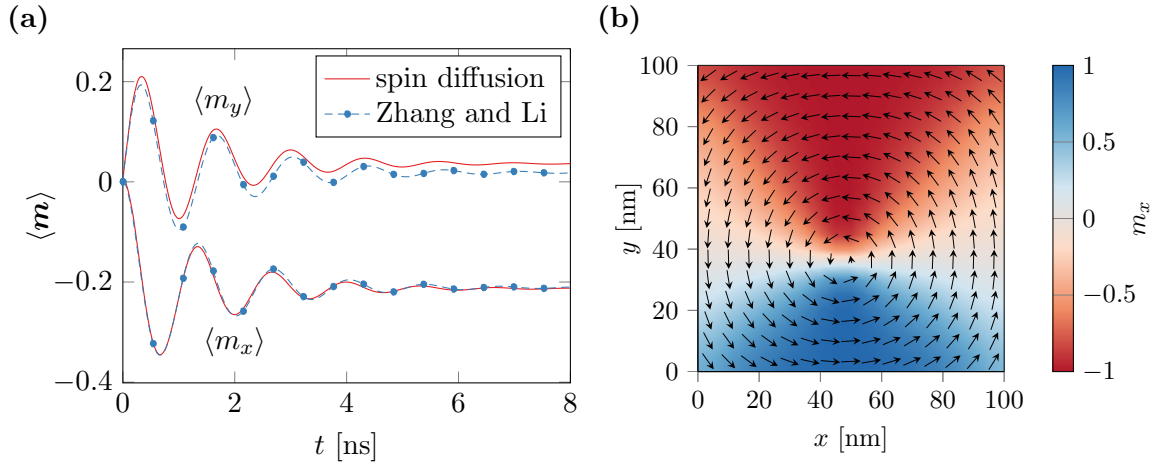


Figure 7: Results for the μ Mag standard problem #5. (a) Time evolution of the spatially averaged magnetization compared to a finite-difference simulation according to Zhang and Li. (b) New equilibrium position of the magnetization.

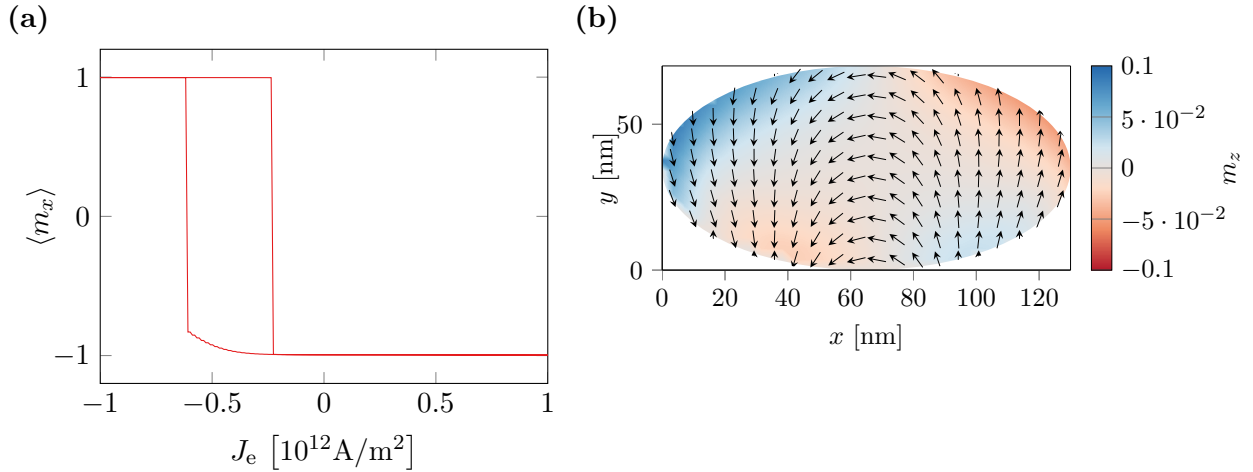


Figure 8: Current hysteresis of a permalloy multi-layer structure. (a) Averaged x -component of the magnetization in the magnetic free layer. (b) Magnetization configuration in the free layer during switching.

Figure 8b shows the magnetization configuration of the free layer during switching. Note that the out-of plane component is small compared to the in-plane component, which is a consequence of the shape anisotropy caused by the small thickness of the layer. The out-of-plane component of the torque as predicted by the spin-diffusion model is compensated by the shape anisotropy as soon as the magnetization is driven slightly out of plane. This may serve as an justification for the missing out-of-plane spin-torque component in the model of Slonczewski.

6 Conclusion

The presented method for the solution of the Landau-Lifshitz-Gilbert equation including spin-torque effects is able to describe both the spin transport in multilayer structures as well as current driven domain-wall motion. The spin torque in multilayers as predicted by Slonczewski is essentially reproduced except for an out-of-plane component that is not present in the model by Slonczewski. However, the out-of-plane component is shown to play an inferior role in typical multilayer structures since it is usually almost completely compensated by shape anisotropy effects. For the description of current-driven domain-wall motion the presented method is compared to a simplified model by Zhang and Li and shows a good agreement. Small deviations can be explained by diffusion terms that are omitted in the simplified model. While the present method is able to resolve the temporal evolution of the spin accumulation exactly it can also be used for an adiabatic description since the time integrator for the spin accumulation behaves very well even for large time steps.

Acknowledgements

The financial support by the Austrian Federal Ministry of Science, Research and Economy and the National Foundation for Research, Technology and Development as well as the Austrian Science Fund (FWF) under grant W1245, the innovative projects initiative of Vienna University of Technology, and the Royal Society under UF080837 is gratefully acknowledged.

References

- [1] S. S. Parkin, M. Hayashi, and L. Thomas, “Magnetic domain-wall racetrack memory,” *Science*, vol. 320, no. 5873, pp. 190–194, 2008.
- [2] M. Hosomi, H. Yamagishi, T. Yamamoto, K. Bessho, Y. Higo, K. Yamane, H. Yamada, M. Shoji, H. Hachino, C. Fukumoto, *et al.*, “A novel nonvolatile memory with spin torque transfer magnetization switching: Spin-RAM,” in *Electron Devices Meeting, 2005. IEDM Technical Digest. IEEE International*, pp. 459–462, IEEE, 2005.
- [3] J. C. Slonczewski, “Current-driven excitation of magnetic multilayers,” *Journal of Magnetism and Magnetic Materials*, vol. 159, no. 1, pp. L1–L7, 1996.
- [4] J. C. Slonczewski, “Currents and torques in metallic magnetic multilayers,” *Journal of Magnetism and Magnetic Materials*, vol. 247, no. 3, pp. 324–338, 2002.
- [5] L. Berger, “New origin for spin current and current-induced spin precession in magnetic multilayers,” *Journal of Applied Physics*, vol. 89, no. 10, pp. 5521–5525, 2001.
- [6] S. Zhang, P. Levy, and A. Fert, “Mechanisms of spin-polarized current-driven magnetization switching,” *Physical review letters*, vol. 88, no. 23, p. 236601, 2002.

- [7] A. Shpiro, P. M. Levy, and S. Zhang, “Self-consistent treatment of nonequilibrium spin torques in magnetic multilayers,” *Physical Review B*, vol. 67, no. 10, p. 104430, 2003.
- [8] S. Zhang and Z. Li, “Roles of nonequilibrium conduction electrons on the magnetization dynamics of ferromagnets,” *Physical Review Letters*, vol. 93, no. 12, p. 127204, 2004.
- [9] C. Abert, G. Hrkac, M. Page, D. Praetorius, M. Ruggeri, and D. Suess, “Spin-polarized transport in ferromagnetic multilayers: An unconditionally convergent FEM integrator,” *Computers & Mathematics with Applications*, vol. 68, no. 6, pp. 639 – 654, 2014.
- [10] C. J. García-Cervera and X.-P. Wang, “Spin-polarized currents in ferromagnetic multilayers,” *Journal of Computational Physics*, vol. 224, no. 2, pp. 699–711, 2007.
- [11] F. Alouges and P. Jaisson, “Convergence of a finite element discretization for the Landau–Lifshitz equations in micromagnetism,” *Mathematical Models and Methods in Applied Sciences*, vol. 16, no. 02, pp. 299–316, 2006.
- [12] P. Goldenits, G. Hrkac, D. Praetorius, and D. Suess, “An effective integrator for the Landau-Lifshitz-Gilbert equation,” in *Proceedings of Mathmod 2012 Conference*, 2012.
- [13] C. Abert, L. Exl, F. Bruckner, A. Drews, and D. Suess, “magnum. fe: A micromagnetic finite-element simulation code based on FEniCS,” *Journal of Magnetism and Magnetic Materials*, vol. 345, pp. 29–35, 2013.
- [14] “magnum.fe.” <http://micromagnetics.org/magnum.fe>.
- [15] A. Logg, K.-A. Mardal, G. N. Wells, *et al.*, *Automated Solution of Differential Equations by the Finite Element Method*. Springer, 2012.
- [16] C. Abert, L. Exl, G. Selke, A. Drews, and T. Schrefl, “Numerical methods for the stray-field calculation: A comparison of recently developed algorithms,” *Journal of Magnetism and Magnetic Materials*, vol. 326, pp. 176–185, 2013.
- [17] X. Brunotte, G. Meunier, and J. Imhoff, “Finite element modeling of unbounded problems using transformations: a rigorous, powerful and easy solution,” *IEEE Transactions on Magnetics*, vol. 28, no. 2, pp. 1663–1666, 1992.
- [18] D. Fredkin and T. Koehler, “Hybrid method for computing demagnetizing fields,” *Magnetics, IEEE Transactions on*, vol. 26, no. 2, pp. 415–417, 1990.
- [19] W. Smigaj, S. Arridge, T. Betcke, J. Phillips, and M. Schweiger, “Solving boundary integral problems with BEM++,” *ACM Transactions on Mathematical Software*, 2012.
- [20] J. Xiao, A. Zangwill, and M. Stiles, “Boltzmann test of Slonczewskis theory of spin-transfer torque,” *Physical Review B*, vol. 70, no. 17, p. 172405, 2004.
- [21] “µMAG standard problem #5.” <http://www.ctcms.nist.gov/~rdm/std5/spec5.xhtml>.
- [22] “MicroMagnum.” <http://magnum.physnet.uni-hamburg.de>.